ACTA ACUSTICA UNITED WITH ACUSTICA
Vol. 90 (2004) 590 – 599

Contemporary Generalized Normal Mode Violin Acoustics

George Bissinger
Physics Department, East Carolina University, Greenville, NC 27858, USA. bissingerg@mail.ecu.edu

Summary
The acoustic properties of a violin can be analyzed in terms of its normal modes by incorporating mode radiativity in addition to the usual vibratory properties. A normal mode database that includes qualitative evaluations as well lends itself to examining aspects of violin dynamics related to quality classes such as "good" or "bad", a relatively straightforward matter for violinists, but much more problematic scientifically. Since the low-lying "signature" modes have shown no robust quality differentiation, our normal mode acoustics investigations move to general aspects of violin acoustics using band-average and trendline quantifiers covering the entire sound spectrum. Initially, understanding the fundamental vibrational energy loss behaviors is of most interest. For a violin suspended "free-free" both total and radiation damping trendlines differ between "good" and "bad" quality classes, but no significant difference was found in the (aggregated) internal damping. Differences between the fraction-of-vibrational-energy-radiated F_{RAD} can be estimated straightforwardly for "good-bad" quality classes from the radiation-total damping ratio, sidestepping the intermediate bridge-corpus energy transfer, (i.e., a "bridge-less" violin). Computing F_{RAD} up to 8 kHz reveals: (1) little overall difference between "good" and "bad" violins, and (2) a relative enhancement of radiation in the 3 kHz region for "good" violins due to a shift in effective critical frequency, boosted even further by holding/bowing the violin.

PACS no. 43.75.De, 43.40.At

1. Introduction

For those interested in the practical (i.e., material-based) reasons why violins sound the way they do when played, the importance of the violin being a linear structure cannot be overstated. Linear means that, in addition to the linear relationship between applied force and system response, there is a fundamental mathematical-physical link between the materials used in its construction, including the actual physical shape of these materials (and how they are joined), and the dynamic vibratory properties of the violin. Because the acoustic radiation from the violin depends directly on how it vibrates, its radiative properties can be expressed in a normal mode milieu also. Our discussion of various normal mode properties here deals both with facets particular to individual modes, and generalized aspects arising from band-averages and trendline analysis.

Analysis of the low-lying (below 700 Hz), readily identifiable "signature" modes for 12 violins – the cavity modes A0 and A1, and the corpus mode CBR (C2)[1], and the acoustically important first corpus bending modes $B1^-$ (T1), $B1^+$ (C3) – revealed no robust discriminator between "good-bad" quality classes [1]. Among the properties examined were normal mode mobility, radiativity, averaged directivity (top/back hemisphere ratio), frequency, total damping, radiation efficiency/damping, aggregate internal (material) damping and fraction-of-vibrational-energy-radiated F_{RAD}. Within error the $B1^-$ and $B1^+$ modes both radiated equally well. Individually they showed no significant difference in frequency or radiativity, F_{RAD} was similar for "bad" and "good" violins, and the averaged directivity was insensitive to quality.

The frequency of the very weakly radiating CBR mode, and the difference between the $B1^-$ and the CBR mode frequencies were the only – just barely significant – correlations found. Given such an inconclusive result for the signature modes, which cover such a small fraction of the violin's overall range, the most promising extension of our generalized normal mode methodology appears to be analyzing violin dynamics up to and beyond the frequency range where the ear is most sensitive. The fact that the analysis must be statistical offers an alternative, complementary approach to understanding violin sound.

2. Normal mode quantifiers

Our generalized normal mode acoustic approach relies on experimental analysis to determine the *mechanical response* (here mobility, $Y(\omega)$ = velocity/Force, (m/s)/N at over 550 points over the violin, including top and back plates, ribs, tailpiece, neck-fingerboard and bridge sub-

Received 18 December 2003,
accepted 30 May 2004.

[1] The Jansson mode labeling in parentheses.

structures), and *acoustic response* (here radiativity [2], $R(\omega)$ = pressure/Force (Pa/N) measured in the far-field in an anechoic chamber at 266 microphone positions over a complete sphere ($r = 1.2$ m) centered on the top plate midway between the bridge feet, with an angular spacing of 15 degrees). The mobility and radiativity were measured simultaneously, using a zero-mass-loading excitation (force hammer striking bridge corner on violin G string side, parallel to plane of violin and bridge) and surface normal response setup (scanning laser Doppler vibrometer), to guarantee that they shared the same excitation force. This combination vibration-radiation measurement greatly enhances and broadens our understanding of the violin's dynamic behaviors. A plot with typical top + back, ribs, tailpiece, neck-fingerboard and bridge rms mobilities below 1 kHz is shown in Figure 1 (contains all the signature modes). For the first time such a mechanical response plot can be accompanied by the rms radiativity $\langle R\rangle$ averaged over all 266 microphone positions, and an rms directivity $\langle D\rangle$, computed from the top-back hemisphere radiativity ratio [3] ($\langle..\rangle$ indicates root-mean-square (rms) averaging).

The addition of radiativity measurements to vibration measurements boosts the number of individual normal mode "quantifiers" from 6 to at least 15 [1]. Six are due to vibrational measurements only, six are due to radiation only, and three require a combination of the vibration and radiation measurements. Since some of these are entirely new quantities a list with symbol for each follows:

Normal Mode Quantifiers

1. Frequency f (or angular frequency ω),
2. Total damping $\zeta_{\rm tot}$ (in percent of critical, $\%crit$),
3. Bridge to violin transfer functions $Y(\omega)$; top, back, ribs, bridge, tailpiece, neck-fingerboard (>550 pts).
4. Mode shape $\{u\}$,
5. Mode character; e.g., cavity (interior air), corpus (top + ribs + back), or substructure (tailpiece, bridge, or neck-fingerboard), necessary for mode counting.
6. Bridge-corpus (top + ribs + back, area-weighted) rms mobility $\langle Y(\omega)\rangle$; squared gives overall measure of energy transfer from bridge to violin corpus. (Unless specifically noted in text this rms quantifier is always bridge-corpus.)
7. Radiativity $R(\omega)$; far-field, bridge-to-radiation-field transfer function at 266 points over sphere.
8. Radiation pattern $\{\Psi\}$ based on the radiativity profile around violin.
9. Rms radiativity over sphere $\langle R(\omega)\rangle$; squared gives overall measure of energy transfer from bridge to acoustical farfield.
10. Averaged directivity $\langle D(\omega)\rangle = \langle R_{\rm top}\rangle / \langle R_{\rm back}\rangle$; unitless, used as a simple measure of the rms radiativity ratio in the top $\langle R_{\rm top}\rangle$ and back $\langle R_{\rm back}\rangle$ hemispheres (exactly in-plane radiativities omitted).
11. Radiation efficiency $R_{\rm eff}$; unitless, requires $\langle R\rangle$, $\langle Y_{\rm corpus}\rangle$, radiating area, but independent of mode frequency.

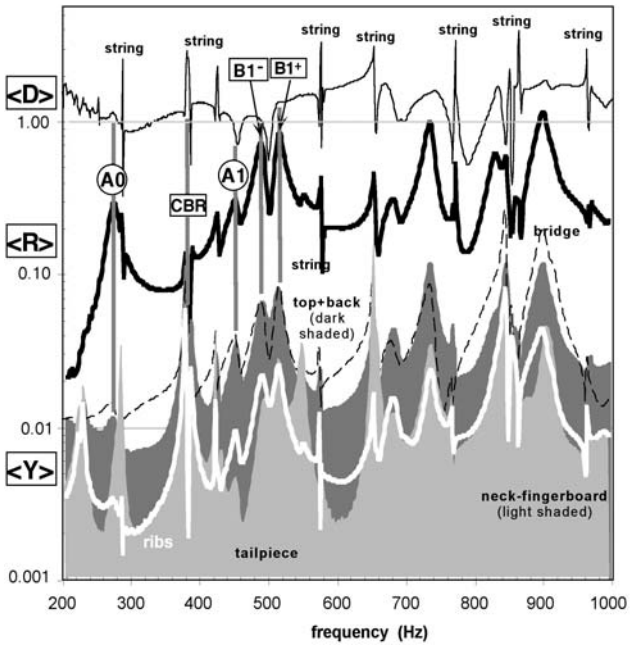

Figure 1. Rms mobility $\langle Y\rangle$ (m/s/N) for violin substructures (lowest sets of curves): top + back (dark shade), ribs (white line), bridge (dashed line), neck-fingerboard (light shade), tailpiece (solid line); radiativity (Pa/N) over sphere $\langle R\rangle$ (center heavy line); directivity $\langle D\rangle$ (unitless) (top line). Signature modes labeled, along with narrow G-D-A-E string harmonics.

12. Radiation damping $\zeta_{\rm rad}$ ($\%crit$); computed from the radiation efficiency, explicitly includes mode frequency and violin mass.
13. Internal damping $\zeta_{\rm int}$ ($\%crit$); computed from total minus radiation damping.
14. Fraction-of-vibrational-energy-radiated $F_{\rm RAD} = \zeta_{\rm rad}/\zeta_{\rm tot}$; unitless, follows radiative energy flow from vibrating violin.
15. Fraction-of-acoustic-energy-from-f-holes F_f ; unitless, measured via near-field acoustic holography techniques [4].

These mode quantifiers individually, or in concert via band-averages or trendlines, constitute a parameter set capable of a) tracing the energy flow through the violin from bridge to corpus and from corpus to sound, b) estimating a critical frequency for a complex structure, and c) simulating the sound of a violin.

If the frequency range is restricted to the approximate range of the violin sound, about 8 kHz, all the dynamic properties can be expressed reasonably well by the sum of contributions from a certain, relatively small, number of normal modes (always fewer than 100 up to 4 kHz – 12 violin sample), with magnitudes that depend directly on how strongly each mode was excited by striking the bridge, or bowing the string, or some other means of excitation.

3. The "Violin Equation"

The normal mode attributes of frequency, damping, shape, and radiation efficiency, plus excitation-from-the-bridge

strength are sufficient to generate a mathematical expression to simulate an averaged-over-sphere, simplified violin sound. This simplified equation for acoustic intensity (expressed without summation over the various normal modes and lacking relative phases), which follows the major energy flow path from the string through the bridge to the violin to the acoustic field, can be written as [3],

$$I(\omega) \propto F^2(\omega)\,\langle Y^2(\omega_i)\rangle\,R_{\mathrm{eff}_i}. \tag{1}$$

The acoustic intensity is proportional to squared sound pressure, $I(\omega) \propto p^2$. On the right hand side, the first term is the energy input to the bridge (typically a sawtooth forcing function). The second term is the corpus mobility transfer function (mean-square values over the corpus), that is a measure of how effectively the energy input at the bridge is transferred to each corpus normal mode. The third term is the radiation efficiency (or ratio, since it is normalized to radiation from a baffled piston), a normal mode parameter that intermediates the conversion of corpus vibrational energy into acoustic energy (averaged over a sphere).

Expressing the energy output as the product of two sequential, independent, vibration and radiation parts helps expose a fundamental physical basis for the inability to work backwards from the sound of the violin to the mechanical construction, viz., given $I(\omega)$ how do we determine $Y(\omega)$ (or R_{eff} for that matter) separately? Analysis of even a normal-mode-based acoustic energy output alone can never lead to materials or construction details of the violin.

4. Radiation efficiency

Radiation efficiency (or ratio) R_{eff} is a dimensionless quantity that relates the radiation for each normal mode relative to a baffled piston of the same area and same mean-square velocity. For the violin it was computed mode-by-mode from [5],

$$R_{\mathrm{eff}} = \frac{1}{\rho^2 c^2}\frac{A}{S}\frac{\langle p^2\rangle}{\langle v^2\rangle}, \tag{2}$$

where ρ_0 is the density of air, c the speed of sound, A the area of the measurement microphone sphere (18.1 m^2), S the surface area of the corpus ($\approx$0.13 m^2), and $\langle p^2\rangle$ and $\langle v^2\rangle$ are the mean-square pressures/velocities over the microphone sphere/corpus. Our radiativities and mobilities, measured simultaneously, substitute for $\langle p^2\rangle$ and $\langle v^2\rangle$ in the ratio. Equation (2) has a certain amount of approximation in its application. The $\langle p^2\rangle$ term is really for radiation from the entire violin, and the area S is really the entire violin area. Fortunately both readily reduce to the corpus values if the mean-square terms are expanded into corpus plus substructure contributions. The $\langle p^2\rangle$ term in equation (2) is the sum of contributions from the corpus and smaller substructures of the violin, viz.,

$$\langle p^2_{\mathrm{violin}}\rangle = \langle p^2_{\mathrm{corpus}}\rangle + \langle p^2_{\mathrm{sub}}\rangle, \tag{3}$$

and since radiation was observed only from the corpus (see Figure 1 for rms mobilities and radiativities for modes $<$1 kHz), substructure contributions to equation (3) are negligible [6], giving

$$\langle p^2_{\mathrm{violin}}\rangle \approx \langle p^2_{\mathrm{corpus}}\rangle. \tag{4}$$

Similarly the $S\langle v^2\rangle$ terms in equation (2) can be written in an area-weighted form, i.e.,

$$S_{\mathrm{violin}}\langle v^2_{\mathrm{violin}}\rangle = \left\langle S_{\mathrm{corpus}} v^2_{\mathrm{corpus}} + \sum_{\mathrm{sub}} S_{\mathrm{sub}} v^2_{\mathrm{sub}} \right\rangle. \tag{5}$$

Because the substructure normal mode contributions are negligible, due both to their much smaller areas and to their much diminished rms velocities relative to the corpus, equation (5) reduces to

$$S_{\mathrm{violin}}\langle v^2_{\mathrm{violin}}\rangle \approx S_{\mathrm{corpus}}\langle v^2_{\mathrm{corpus}}\rangle. \tag{6}$$

The radiation efficiency is a crucial normal mode quantifier for the following reasons: a) typically R_{eff} is low when the sound wavelength is much larger than the dimensions of the source, rising to a plateau value of 1 for structures when the bending wave velocity in the structure makes the transition from subsonic to supersonic, b) R_{eff} is used to compute the radiation damping, and c) the trendline equation for R_{eff} can be used to estimate the critical frequency by solving the equation at $R_{\mathrm{eff}} = 1$ [6]. These experimental estimates of the critical frequency bypass an inherently difficult part in understanding violin acoustics, viz., computing the critical frequency for such a complex structure. Analytical expressions exist for simple geometries only. Additionally there are some possibly crucial structural acoustics considerations if the violin does indeed have radiative similarities to the thin-walled cylinder [5, 6]. Consequently we label our estimate of the critical frequency as an "effective" critical frequency.

The first two terms in equation (1) comprise the energy input to the bridge from the string vibrations and its conversion into violin vibrational energy; radiative-loss paths can be parameterized straightforwardly by the third term, mode radiation efficiencies. However a more general and equally fundamental characterization of just the energy loss path is through the total, radiation and internal (aggregate) damping properties for the violin.

5. Signature to statistical

The VIOCADEAS database includes normal-mode vibration and acoustics measurements and materials information on violins of widely varying quality [1, 7] as well as normal mode analysis of a Hutchins-Schelleng violin octet [8, 9]. The octet shapes were scaled from the violin, and essentially all were built with the same basic materials. Hence even over the enormous size range of the octet certain low-lying modes - where wavelength greatly exceeded small-scale variations in material properties - were always similar to those observed in violins. These "signature" modes fall below 700 Hz for the violin, usually lie in

the same order, are generally well separated and hence fit well by any modal analysis program, and blessed with simple, easily identifiable shapes. They offer the only practical instances where inter-violin individual normal mode comparisons are valid.

Above this region smaller-scale material property or constructional variations start to influence the vibratory characteristics of each violin, and mode shapes become less easily identifiable. Modal overlap also becomes more significant, and fitting programs usually need to fit more than a single mode in a band, reducing the reliability of individual mode damping values although the average damping in such a band should still be reliable. Such behaviors are better handled in statistical ways.

This evolution from "signature" to "statistical" is actually quite convenient, restricting mode comparisons to a reasonable number of individual modes at frequencies below 700 Hz for consistent inter-violin comparisons. Above 1 kHz band-average comparisons are more fruitful. Finally, trendlines that can realistically cover the range up to 8 kHz, a practical range for violin sound, offer additional highly valuable information.

6. Quality differentiators

Each violin can now be parameterized by at least 20 different measurable normal-mode quantifiers, some particular to an individual mode as noted above, some averaged over 250-Hz bands, some based on trendlines through the band-average data. Adding a quality rating provides an entirely new "coordinate axis" to consider. By taking the three best ("good") and three worst ("bad") of our quality-rated violins, averaging their relevant normal mode quantifiers, and then comparing these quantifiers, possibly a robust normal mode differentiator between quality classes might be expected to appear [1].

As noted earlier, however, only one signature mode frequency and one frequency difference barely reached one standard deviation significance, hardly robust. These signature mode frequencies nonetheless are presently the preeminent quantifiers for violins!

Since particular signature mode properties appear not to be robust quality descriptors at this juncture, we shift to a more general band-average and trendline-based analysis. Our generalized normal mode analysis now evolves to more abstract, but equally fundamental, tracing of the energy flow out of the vibrating violin via modal-average damping analysis.

7. Damping

Damping measurements help quantify how the violin loses its vibrational energy. There are only three possible energy loss paths: internal (heat), acoustic radiation, and support fixture. The violin support fixture was purposely designed to provide near free-free support conditions while being acoustically transparent [10]. Being able to neglect energy loss paths other than to internal (heat) and acoustic radiation was a crucial prerequisite for estimating the internal damping from the measured total and radiation dampings.

7.1. Total damping

To make proper damping measurements on the violin, i.e., to measure the violin – and not the violin plus its support fixture – it is essential to isolate the violin from its support fixture to the maximum extent practicable. The violin (sans chin and shoulder rests) was suspended in an anechoic chamber by two low-mass elastics under the incurved portions of the lower-bout end of the C-bouts. This support fixture approximates a "free-free" support condition, with very low damping losses ($\leq 5\%$ of total damping) [10].

The total damping measured for the violin, ζ_{tot}, includes the true internal (heat) losses as well as losses to acoustic radiation and the support fixture. i.e.,

$$\zeta_{\mathrm{tot}} = \zeta_{\mathrm{int}} + \zeta_{\mathrm{rad}} + \zeta_{\mathrm{fix}}. \tag{7}$$

Since the support fixture damping is negligible,

$$\zeta_{\mathrm{tot}} \approx \zeta_{\mathrm{int}} + \zeta_{\mathrm{rad}}. \tag{8}$$

The total damping for each mode (in percent of critical damping – $\%crit$) was taken from a global (average-over-the-violin) fit to the mobility spectra. These $\%crit$ damping values are easily turned into Q values (Q = energy stored/energy lost per cycle) by using $\%crit = 50/Q$. These violin damping values can vary widely mode-to-mode but always show an overall drop-off trend as frequency increases [7].

A scatter plot of ζ_{tot} for over 400 modes up to 4 kHz is shown in Figure 2. The plot was specifically chosen to be a log–log plot so that if the data show linear trends then the parametric dependence would be power-law, viz., $\zeta_{\mathrm{tot}} = Cf^x$. Even with the data spray seen in Figure 1, a linear drop off with increasing frequency is a reasonable representation of what is observed. While most of the mode dampings shown are for the corpus modes, a few substructure modes (neck-fingerboard, tailpiece, bridge – but not strings) have been left in the data array to show their lower damping values (hatched area). This lower damping was one defining characteristic of substructure modes, at least partly due to the fact that none of them radiated significantly. Also included are averaged damping results for the cavity mode A0, easily the highest value for each violin.

The large squares shown in Figure 2 are corpus-only 250-Hz-band modal averages. These band averages both simplify the data analysis and provide a standard deviation as a numerical measure of the range of damping values intra-band. This standard deviation (a typical example is shown) is not an experimental error for the total damping or radiation efficiency/damping measurements, both of which have experimental errors of approximately $\pm 10\%$ for isolated modes.

The fall-off in violin total damping differs noticeably from measured damping trends for the isolated top and

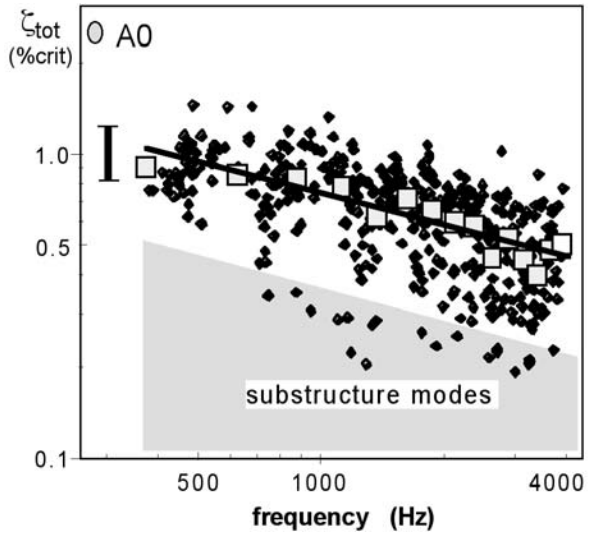

Figure 2. Total damping ($\%crit$) collected for nine violins up to 4 kHz. Shaded region highlights substructure modes. Boxes show 250-Hz-band-averages (typical standard deviation shown for one band only); trendline power-law fit to band-averaged points. A0 result (averaged) shown as oval disk (spread for standard deviation of f and $\zeta_{\rm tot}$).

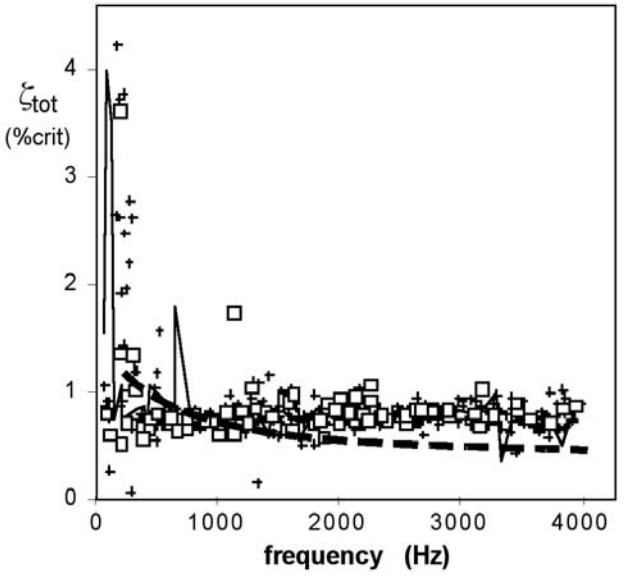

Figure 3. Comparison of total damping trends of seven spruce top plates (+, including one varnished), two maple back plates (□, one flat violin-shaped spruce plate with f-holes (thin solid line). Superimposed violin power-law trendline from Figure 2 (dashed thick line).

back plate substructures. Measurements of total damping for 7 top plates, with and without varnish, are shown in Figure 3. These show a wide range of damping values for the lowest modes, but relatively little change at higher frequencies, overall being almost constant up to 4 kHz, implying $x \approx 0$. This trend for arched top and back plates with a midline glue joint is consistent with measurements for individual strips, or other very simple geometry samples, but contrasts sharply with the downward violin trends shown superimposed on the substructure results in Figure 3. Power law fits to all violins gave $x = -0.34 \pm 0.05$; "good" violins had $x = -0.29 \pm 0.05$ while the "bad" had $x = -0.45 \pm 0.05$, a significant difference [6]. It is not yet clear where this difference originates however, i.e., is the internal (aggregate material) damping higher for "good" violins, or "bad"? Or is the radiation damping higher? Or are both different?

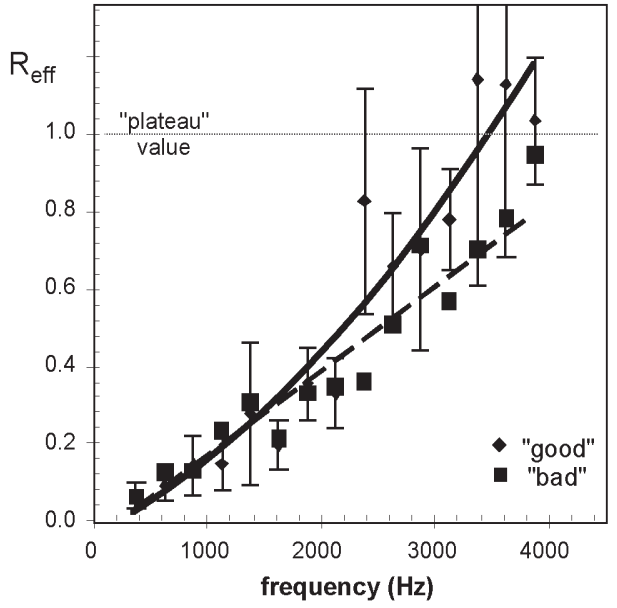

Figure 4. 250-Hz-band modal-average radiation efficiency for "good" and "bad" violins, with trendlines (range standard deviation for "good" only).

7.2. Radiation damping

Other than the obvious – radiation from the violin must be important because this is what we hear – just how important a contribution is radiation damping to the overall total damping? To assess this radiation damping $\zeta_{\rm rad}$ ($\%crit$) was computed from the radiation efficiency $R_{\rm eff}$, for each mode of the violin, using the equation [7],

$$\zeta_{\rm rad} = 50 \frac{\rho_0 c}{2\pi} \frac{S}{M} \frac{R_{\rm eff}}{f}, \tag{9}$$

where M is the mass of the violin, nominally 0.43 kg, f is the mode frequency, and S is the surface area of the corpus (see section 4), nominally 0.13 m^2. The inverse dependence on violin mass (not expected for internal damping) is important because – all other things being equal (although being wood, they never are) – the lighter the violin the higher its radiation damping, across the acoustic spectrum.

Experimental 250-Hz-band averaged $R_{\rm eff}$ values for "good" and "bad" violins are shown in Figure 4. The more rapid rise for the "good" violins is apparent. The trendlines shown are polynomial fits of order two or one – where the minimum order with equivalent r-correlation coefficient was always chosen [6]. All r-values exceeded 0.8. These trendlines for $R_{\rm eff}$ were also used in equation (9) to compute $\zeta_{\rm rad}$ trendlines.

It is helpful to understand both the general behavior of $R_{\rm eff}$ and $\zeta_{\rm rad}$, and thus how $\zeta_{\rm rad}$ can affect violin sound. Figure 5 shows a stylized version of the general behaviors of $R_{\rm eff}$ and $\zeta_{\rm rad}$ with increasing frequency. Of special importance is the transition region at the critical frequency as $R_{\rm eff}$ transitions to its plateau value and where the rising behavior of $\zeta_{\rm rad}$ suddenly switches to a $1/f$ falloff, producing a "knee" in the curve. This knee region enhances violin radiation near the critical frequency.

Estimating critical frequencies by solving the trendline equation for $R_{\rm eff} = 1$, we find critical frequencies of about 3.4 kHz for the "good" and 4.8 kHz for the "bad" violins [6]. A varying critical frequency means that the knee in the radiation damping curve moves, while the overall magnitudes and shape are maintained. Our generalized normal-mode acoustics approach then attaches the $R_{\rm eff} = 1$ plateau at the knee, completing the $R_{\rm eff}$ trendline over the entire violin range. The "good-bad" critical frequency shift changes the position of the knee in the radiation damping curve, implying that the spectral balance of sound changes between violin quality classes. Before this matter can be addressed an additional step – computing the internal damping – is necessary.

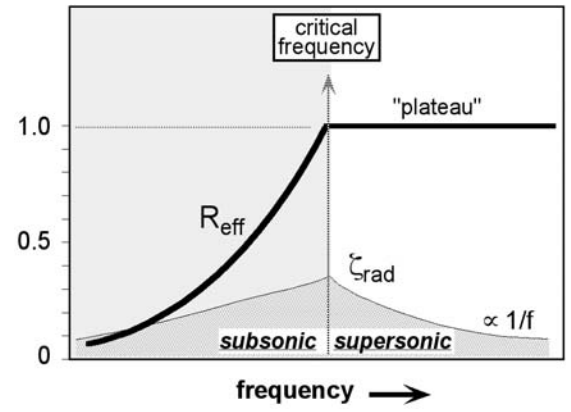

Figure 5. Generalized radiation efficiency (dimensionless - solid curve) and radiation damping ($\%crit$ - filled curve) trends for violins (realistic values - both parameters).

7.3. Internal damping

With $\zeta_{\rm rad}$ and $\zeta_{\rm tot}$ it is possible to compute both the internal damping of the violin, and the fraction-of-vibrational-energy-radiated $F_{\rm RAD}$, mode-by-mode or with trendlines. 'True' internal (material) damping is a new quantity for the violin, due to the fact that the measured total damping for a violin must have radiation damping subtracted to extract it. Previous material damping measurements often used small simple structures with little radiating area, hence the material damping values were much closer to the measured total damping. On the other hand our measurements are all for an assembled violin, and hence are really an aggregate internal damping. (Note that there might be some contribution from sound absorption internally.) With our $\zeta_{\rm rad}$ and $\zeta_{\rm tot}$ results it is straightforward to compute an aggregate internal damping [11], viz.,

$$\zeta_{\rm int} \approx \zeta_{\rm tot} - \zeta_{\rm rad}. \qquad (10)$$

The internal damping computed from equation (10) is shown in Figure 6 for the 250-Hz-band-averaged dampings for "good" and "bad" violins. Each data point has a propagated 'error' bar derived from the standard deviations representing ranges of total and radiation damping. Note that the total damping and radiation damping have estimated *experimental* errors of ±10% for isolated modes, approximately a factor of 3 smaller than the average intra-band standard deviations. Hence computed 'errors' are dominated by intra-band *variations*, not experimental errors. Damping difference 'errors' will appear correspondingly larger.

The power law behavior observed in Figure 2 has been extended to the internal damping both because it is a reasonable parameterization of the experimental data and because it is well behaved outside the fit region. This provides a reasonable basis to extrapolate up to 8 kHz to cover the important acoustic range of the violin. The power law fits for the "good" and "bad" violin are superimposed on 250-Hz-band modal average results in Figure 6. Within the internal damping 'errors' it is clear that there is no significant difference between the "good" and "bad" violin internal dampings for these relatively modern instruments, hence $x = -0.68 \pm 0.12$ was chosen for the power law exponent for both [6]. It is entirely possible of course that measurements on very old violins could give a different internal damping result.

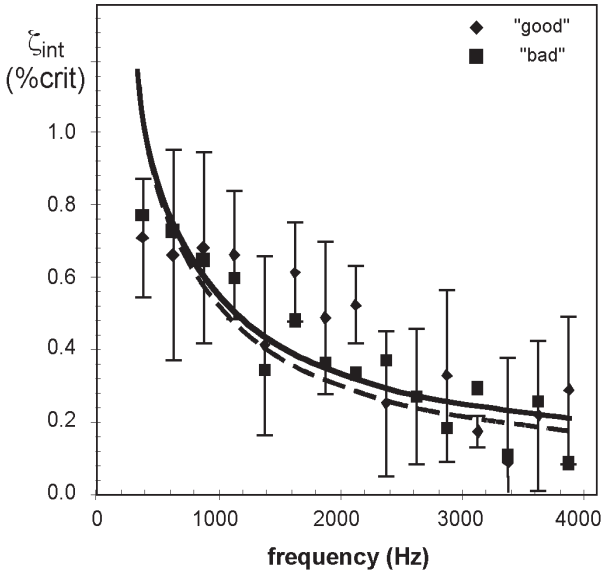

Figure 6. 250-Hz-band modal-average internal dampings for "good" and "bad" violins from total and radiation damping differences (range standard deviation for "good" only); power law trendlines (solid "good", dashed "bad").

Would it necessarily be expected that the internal (material) damping should be different between "good" and "bad" violins? Although modern violinmaking practice seems to indicate that top/back plate wood should ring when struck, Curtin has noted that old Italian violins do

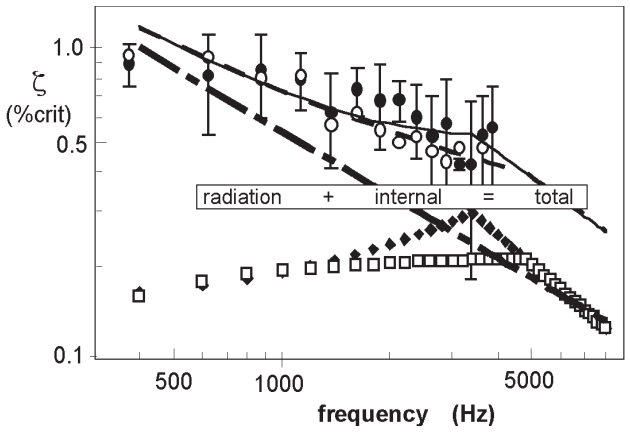

Figure 7. Summary plot of radiation ('good' ◆,'bad □), internal (— - —), and total ('good' ——, 'bad – – –) damping trendlines. Experimental total damping for 'good' (●) and 'bad' (○) violins shown for comparison (from [6]).

not have this response, that many of their plates sound much more highly damped than modern instruments when tapped [12]. Curtin's personal experience, the observed lack of differentiation in internal damping between modern "good" and "bad" violins in our experiments, and simulations of violin sound with varying Q electronic circuits by Mathews and Kohut [13] (where increasing Q from low to high changed the bowed sound from normal violin-like to a "hollow-sounding, uneven instrument"), all lead us to speculate that internal (material) damping is not a robust indicator of quality as long as it is high enough.

Truncated modal analysis of a held/fingered violin by Marshall showed greatly increased total damping relative to the free-free state [14]. His results have been confirmed in our laboratory. This provides evidence that the musician's "support fixture" damping greatly exceeds both the internal and radiation damping components in the total damping (as measured in a free-free setup). Under these circumstances internal damping may make little difference irrespective of its magnitude (within reasonable limits) when the instrument is played. A summary plot of all the damping components is given in Figure 7. The radiation and internal damping are presented as trendlines only, while the total damping trendline, computed from the sum of the internal plus radiation damping trendline values is superimposed on the experimental total damping results for "good" and "bad" violins. The agreement between experiment and total damping trendline is generally quite good.

8. F_{RAD} and the "Bridge-Less" violin

The fraction-of-vibrational-energy-radiated F_{RAD} is an experimental quantifier evolved from other normal mode quantifiers. It is computed simply from our damping results as

$$F_{\mathrm{RAD}} = \frac{\zeta_{\mathrm{rad}}}{\zeta_{\mathrm{tot}}}. \tag{11}$$

Values of F_{RAD} computed from experimental ζ_{tot} and ζ_{rad} 250-Hz-band averages using equation (11) are shown in Figure 8. The difference observed between F_{RAD} for "good" and "bad" violins was not large, indicating that "bad" violins radiate overall just about as effectively as "good" ones, a result consistent with earlier inverse monopole radiativity results of Weinreich below 1 kHz [2]. The damping analysis here however allows absolute experimental comparisons over the entire range of frequencies up to 4 kHz and reasonable extrapolation beyond this range via modal band-average trendline modeling and structural acoustics systematics. Figure 8 also shows that both violin quality classes radiate up to approximately 50% of their vibratory energy. Again, no consideration of how effectively input energy is transferred from the strings to the violin body is possible in our damping analysis since it deals only with vibratory energy loss.

Also note an estimate of F_{RAD} for A0 in Figure 8. Strictly speaking for a cavity mode such as A0 this estimate is really only heuristic and does not attempt to investigate the A0 excitation mechanism for energy transferred from the strings to the corpus to the cavity. This estimate is based entirely on Cremer's computation of radiation and viscous (here taken as "internal") damping losses for A0, which were approximately the same [15], hence $F_{\mathrm{RAD}} \approx 0.5$. Although it might seem that F_{RAD} should be substantially different between the two quality classes since ζ_{rad} is nearly 50% larger for the "good" violins near the critical frequency, ζ_{rad} is also part of ζ_{tot} (as is ζ_{int}) so in the ratio the difference is diminished. This can be seen more easily by rewriting the equation for F_{RAD},

$$F_{\mathrm{RAD}} = \frac{1}{1 + \frac{\zeta_{\mathrm{int}}}{\zeta_{\mathrm{rad}}}}. \tag{12}$$

Examining F_{RAD} behavior using equation (12) with modal averages in each band, it is clear that the ratio of internal to radiation damping is what governs the behavior of F_{RAD}. The internal damping is the same for each band ("good" or "bad"), dominating the total damping up to about 2 kHz. Since the radiation dampings are also very similar below 2 kHz and slowly increasing, F_{RAD} will be very similar below 2 kHz, starting small and slowly increasing. In those regions where $R_{\mathrm{eff}} = 1$ for both violins (the plateau region) the radiation damping in each band is the same, as is the internal damping, so again no differences in F_{RAD} are expected. Only in the region between 2 kHz and the higher critical frequency, where the radiation damping differs the most, should significant F_{RAD} differences occur, i.e., around 3 kHz, the most sensitive region for our hearing.

A heuristic approach to understanding the audible significance of this emphasis around 3 kHz and how important the radiation damping is to its strength begins by modifying equation (1) for simulating violin sound to incorporate F_{RAD}. First, we bypass the bridge-corpus energy transfer term, to eliminate any possible "bridge-hill" influence [16] on the acoustic output of the violin. This modi-

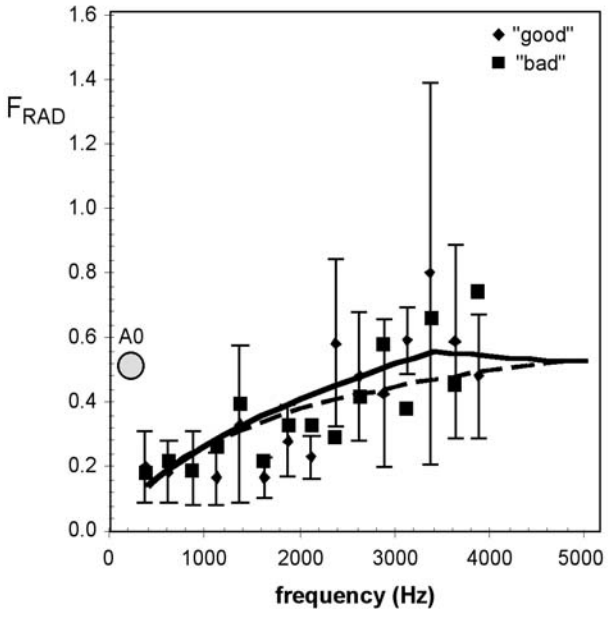

Figure 8. 250-Hz-band modal-average fraction-of-vibrational-energy-radiated for "good" and "bad" violins (standard deviation for F_{RAD}, "good" only). Trendline estimates: "good" (solid line), "bad" (dashed line). Estimate for A0 also shown by shaded circle (see text).

fication entails only setting $\langle Y^2 \rangle = 1$, so that the string energy passes directly to the violin corpus. Second, we note that the input energy $F(\omega)^2$ – once in the corpus - can only be converted to sound or heat. Since F_{RAD} gives the fraction of vibrational energy converted to sound the "bridge-less" violin has a simulated sound [6] that can be expressed as

$$I(\omega) \propto F(\omega) F_{\mathrm{RAD}}. \tag{13}$$

F_{RAD} can now be seen to serve two main functions: (1) it acts as an energy filter that modifies the spectral balance of energy passing through it, irrespective of whether the forcing function is harmonic or noise or some combination thereof, and (2) it is a measure of relative loudness across the acoustic spectrum. These relative aspects are important and the following section extends it from the "free-free" measurement state, to the "held/bowed" playing state where the final judgments are made.

9. Playing the violin

Can our results for a violin suspended in a free-free state offer any insights into the sound of the violin when it is being played? This of course is where the final acoustic judgment is made, and is of the greatest practical importance. We assume that holding/playing does not materially affect the input energy transfer chain string-bridge-corpus term in the violin equation. Marshall had observed little change in mode frequencies and shapes between the free-free and held conditions with fingers and bow touching the strings, but, as expected, considerable decrease in mechanical response was noted, accompanied by very substantial increases in the total damping [14]. Unexpectedly, large support fixture damping effects are significant to the sound in a not very obvious way.

Our F_{RAD} "filter" analysis of the free-free damping is an apt place from which to evolve the effect of holding/bowing. First, it is necessary to understand the effect of holding on the radiation efficiency/damping. Assuming that little change in mode shape occurs [14], since the radiation efficiency is computed from the radiativity/mobility ratio, substantial decreases in mechanical response should be accompanied by similar decreases in acoustic radiation. Hence we argue that no major changes occur in radiation efficiency or radiation damping values, or in the stylized radiation efficiency/damping curves of Figure 5.

Second, our free-free damping analysis concluded that the internal (material) damping was basically the same for "good" and "bad" violins, and it would not be expected to change significantly in the held/bowed state. In light of these considerations we can then conclude that the large observed increase in total damping arises mainly from greatly increased support fixture damping, hence ζ_{fix} can no longer be considered negligible.

With the source of the observed increase in damping settled, approximate experimental estimates of the change in F_{RAD} from "free-free" to "held/bowed" state are now straightforward. In equation (7), the denominator ζ_{tot} will now be dominated by the support fixture damping since $\zeta_{\mathrm{fix}} \gg \zeta_{\mathrm{int}}$ or ζ_{rad}, and we can reasonably assume that ζ_{fix} would be the same for "good" or "bad" violins. Comparing our own zero-mass-loading free-free measurements with those on the same violin held/bowed provided an approximate support fixture-player damping of $\zeta_{\mathrm{fix}} \approx 3\zeta_{\mathrm{int}}$. Also the internal damping, over the range of the violin (see Figure 8), averages about twice as large as the radiation damping, or $\zeta_{\mathrm{int}} \approx 2\zeta_{\mathrm{rad}}$. Combining both factors gives $\zeta_{\mathrm{fix}} + \zeta_{\mathrm{int}} \approx 7\zeta_{\mathrm{rad}}$ so that $\zeta_{\mathrm{tot}} \approx \zeta_{\mathrm{fix}} + \zeta_{\mathrm{int}}$ which is almost a constant (within about 10%), and much larger than ζ_{rad}. For the held/bowed case the maximum value for F_{RAD} is now only about 0.1, predictably much reduced from the free-free case.

Changes in F_{RAD} are really more noteworthy in the "filter" effect than in the fully expected overall drop in F_{RAD}. This can be seen best when the sound is compared by taking a "good-bad" F_{RAD} ratio for free-free and held/bowed violins. Since we can plausibly claim that the forcing function is mostly unaffected by violin quality, computing the "good-bad" ratio for $I(\omega)$ cancels out the forcing function in equation (13), leaving only the F_{RAD} ratio as the determiner of relative sound quality. Two limiting curves are displayed in Figure 9, the F_{RAD} ratio for the free–free case ($f - f$), there the support fixture damping is negligible, computed from

$$\frac{F^{\mathrm{good}}_{\mathrm{RAD}f-f}}{F^{\mathrm{bad}}_{\mathrm{RAD}f-f}} = \frac{\zeta^{\mathrm{good}}_{\mathrm{rad}}}{\zeta^{\mathrm{bad}}_{\mathrm{rad}}} \left(\frac{\zeta^{\mathrm{bad}}_{\mathrm{rad}} + \zeta_{\mathrm{int}}}{\zeta^{\mathrm{good}}_{\mathrm{rad}} + \zeta_{\mathrm{int}}} \right), \tag{14}$$

and the held/bowed case (hb) where $\zeta_{\mathrm{rad}} \ll \zeta_{\mathrm{tot}}$ since support fixture-player damping dominates ζ_{tot}. The result

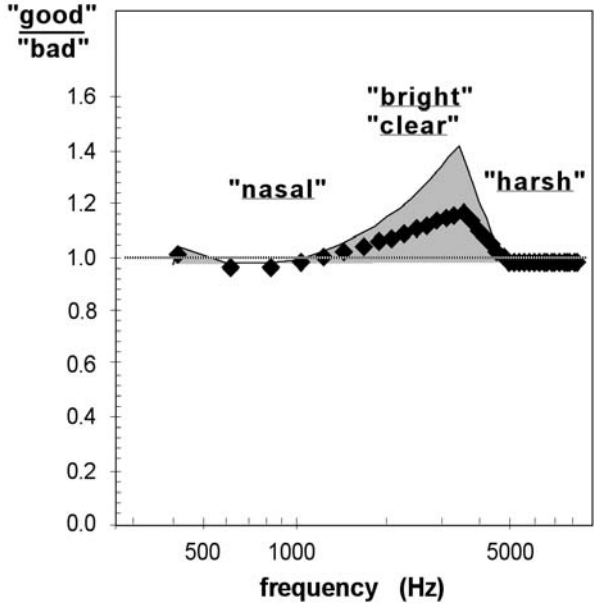

Figure 9. F_{RAD} "good-bad" ratio for free-free (◆) vs. held / bowed (solid, shaded line). Qualitative descriptors for various frequency bands from [17, 18] and [19].

for the held/bowed case, computed in the limit $\zeta_{\mathrm{fix}} \to \infty$, is just

$$\frac{F^{\mathrm{good}}_{\mathrm{RAD}hb}}{F^{\mathrm{bad}}_{\mathrm{RAD}hb}} \approx \frac{\zeta^{\mathrm{good}}_{\mathrm{rad}}}{\zeta^{\mathrm{bad}}_{\mathrm{rad}}}. \tag{15}$$

The violinist's damping is so large, and common to both quality classes (as is the internal damping, which is swamped), that it dominates ζ_{tot}, causing it to cancel in the ratio. This leaves the "good-bad" F_{RAD} ratio for the held/bowed case as the ratio of the good-bad radiation damping.

When held/bowed the F_{RAD} *difference* is emphasized because only radiation dampings – the only damping component that differs between quality classes – remain. Hence sound differences between "good" and "bad" violins appear significantly accentuated by holding and playing the instrument.

As an aid to understanding the acoustic importance of structure seen in the F_{RAD} ratio, Figure 9 also incorporates violin-related psychoacoustic terms from the work of Meinel [17] and Dünnwald [18, 19] to characterize certain sound qualities associated with relative enhancement of acoustic emission in certain frequency regions. F_{RAD} differs most near 3 kHz (due to the knee), also the region in which the ear is most sensitive.

Support fixture damping also offers some insight into why an old, Italian violin whose plates seem so "dead" can actually sound sufficiently loud when played – the increased internal damping does not dominate the total damping.

A brief remark about playing evaluations vs. measurements seems apropos here. Playing "good" and "bad" violins tends to emphasize the purely radiative differences more than any measurement where all extraneous interactions have been purposely minimized. That is, measuring the violin in the free-free state in some sense diminishes the very quality-related differences we would like to measure. This loss of discrimination must be balanced against the understanding gained about the importance of internal material damping to quality. *Internal material damping can now be understood to be relatively unimportant to perceived violin quality.* Future measurement setups might beneficially simulate the violinist's stiffness, mass, and damping support-fixture characteristics when holding the violin if this can be done without interfering with the essential acoustic radiativity measurements.

Of course this discussion does not take into account the substantial decrease in the fraction of acoustic energy radiated, or the effect this has on the perceived sound quality, but frequency placement of the boost, emphasizing as it does the very region that leads to characterization of violin sound as "bright, clear," rather than the less desirable "nasal" or "harsh" appellations lends it additional perceptual weight.

10. *f*-Hole vs. structure radiation

One of the questions that a more comprehensive investigation of violin radiativity must address is the relative contribution of radiation from the *f*-holes vs. the corpus. The first patch near-field acoustic holography (pNAH) measurements on *f*-hole radiation offer a surprising answer [3]. The pNAH technique is an important extension of the general NAH technique. By measuring the near-field pressure over a rectangular grid covering just the region of interest, here the two *f*-hole regions, the NAH formalism [20, 21] can be extended to reconstructing the volume velocity and intensity in the *f*-hole and to computing radiation contributions in the far-field. The pNAH analysis process backtracks the velocity field to the violin surface, allowing isolation of the *f*-hole contribution so radiation from only that portion of the violin can be compared to the overall radiation. This also makes it possible to estimate the relative contributions of corpus and *f*-holes. As expected, A0 radiates only through the *f*-holes. These preliminary results offer insight into how important *f*-hole radiation can be for supposed corpus modes [22], including the acoustically important first corpus bending modes, which radiate quite strongly through the *f*-holes. Although it is not possible to look at corpus mode volume changes as simply forcing air out the *f*-holes except when the wavelength greatly exceeds the dimensions, still this result reveals an interesting new feature of structure modes that should be investigated to understand the overall radiation from the violin.

11. Conclusions

Our investigations have emphasized generalized damping – energy loss – properties of the violin rather than the excitation or radiation properties of the signature modes,

since these latter appear only weakly relevant to quality. This type of analysis has led us to some important general conclusions: (1) internal (aggregate) material damping is not a robust discriminator between "good" and "bad" violins, (2) the critical frequency is significantly different between "good" and "bad" violins, (3) the radiation damping "knee", which occurs at the critical frequency, boosts the acoustic radiation relative to regions above or below it, and (4) the support-fixture damping effects introduced by holding-playing the violin can actually enhance acoustic differences between "good" and "bad" violins, as quantified by F_{RAD}. The latter two conclusions are independent of any bridge-hill or other filter effects related to energy transfer through the bridge into the violin. Detailed examination of generalized excitation effects that might differentiate between quality classes is still in progress.

Acknowledgement

We acknowledge the essential support of the National Science Foundation (DMR-9802656) for this research, and discussions with Drs. Frank Fahy and Jim Woodhouse.

References

[1] G. Bissinger, A. Gregorian: Relating normal mode properties of violins to overall quality: signature modes. Catgut Acoust. Soc. J. (Series II) **4** (37-45) 2003.

[2] G. Weinreich: Violin radiativity: concepts and measurements. Proc. Stockholm Music. Acoust. Conf., Royal Swed. Acad. Mus. **46** (1985) 99–110.

[3] G. Bissinger, J. C. Keiffer: Radiation damping, efficiency, and directivity for violin normal modes below 4 kHz. Acoust. Res. Lett. Online **4** (2003) 7–12. http://ojps.aip.org/ARLO/top.jsp.

[4] E. G. Williams, G. Bissinger: Analysis of the radiation from the violin f-holes using patch near-field acoustical holography. J. Acoust. Soc. Am. **113** (2003) 2314.

[5] F. Fahy: Sound and structural vibration: Radiation, transmission and response. (Academic Press, New York, 1987, paperback) and private communication.

[6] G. Bissinger: The role of radiation damping in violin sound. Acoust. Res. Lett. Online **5** (2004) 82–87. http://ojps.aip.org/ARLO/top.jsp.

[7] G. Bissinger: Relating normal mode properties of violins to overall quality: modal averages/trends. Catgut Acoust. Soc. J. (Series II) **4** (2003) 46–52.

[8] G. Bissinger: Modal analysis of a violin octet. J. Acoust. Soc. Am. **113** (2003) 2105–2113.

[9] G. Bissinger: Wall compliance and violin cavity modes. J. Acoust. Soc. Am. **113** (2003) 1718–1723.

[10] K. Ye, G. Bissinger: Attaining 'free-free' normal mode frequency and damping conditions for the violin. Proc.18th Intern. Modal Analysis Conf.- Soc. Exp. Mechanics, Bethel, CT, 2000, 398–403.

[11] G. Bissinger: Extracting internal damping from total damping and radiation efficiency measurements. Proc. 21st Intern. Modal Analysis Conf.- Soc. Exp. Mechanics (CD only), Bethel, CT, 2003, paper #160.

[12] J. Curtin: Innovation in violinmaking. Proc. Intern. Symp. Musical Acoust., ASA-CAS, 1998, 11–16.

[13] M. V. Mathews, J. Kohut: Electronic simulation of violin resonances. J. Acoust. Soc. Amer. **53** (1973) 1620–1626. recorded examples, "Electronic violin with adjustable resonances", Sound Generation in Winds, Strings, Computers, Royal Swedish Academy of Music No. 29 (1980).

[14] K. D. Marshall: The musician and the vibrational behavior of a violin. Catgut Acoust. Soc. J. **45** (1985) 28–33.

[15] L. Cremer: The physics of the violin. MIT Press, Cambridge, 1984.

[16] E. V. Jansson, B. Niewczyk, L. Frydén: The BH peak of the violin and its relation to construction and function. Proc. 17th Intern. Congr. Acoust., 2001, vol. 4 (Music #7B.14.03), 10–11.

[17] H. Meinel: Regarding the sound quality of violins and a scientific basis for violin construction. J. Acoust. Soc. Am. **29** (1957) 817–822.

[18] H. Dünnwald: Ein erweitertes Verfarhren zur objektiven Bestimmung der Klangqualität von Violinen. Acustica **71** (1990) 269–276.

[19] H. Dünnwald: Deduction of objective quality parameters on old and new violins. Catgut Acoust. Soc. J. (Series II) **1** (1991) 1–5.

[20] E. G. Williams: Fourier acoustics: Sound radiation and nearfield acoustical holography. Academic Press, New York, 1999.

[21] E. G. Williams, B. H. Houston, P. C. Herdic: Fast Fourier transform and singular value decomposition formulations for patch nearfield acoustical holography. J. Acoust. Soc. Am. **114** (2003) 1322–1333.

[22] G. Weinreich, C. Holmes, M. Mellody: Air-wood coupling and the swiss-cheese violin. J. Acoust. Soc. Am. **108** (2000) 2389–2402.